Space-variant filtering for correction of wavefront curvature effects in spotlight-mode SAR imagery formed via polar formatting

Charles V. Jakowatz, Jr., Daniel E. Wahl, Paul A. Thompson, and Neall E. Doren

Sandia National Laboratories
Albuquerque, NM

Abstract

Wavefront curvature defocus effects can occur in spotlight-mode SAR imagery when images are constructed via the well-known polar formatting algorithm (PFA) under certain scenarios that include imaging at close range, use of very low center frequency, and/or imaging of very large scenes. The range migration algorithm (RMA), also known as seismic migration, was developed to accommodate these wavefront curvature effects. However, the along-track upsampling of the phase history data required of the original version of range migration can in certain instances represent a major computational burden. A more recent version of migration processing, the Frequency Domain Replication and Downsampling (FReD) algorithm, obviates the need to upsample, and is accordingly more efficient. In this paper we demonstrate that the combination of traditional polar formatting with appropriate space-variant post-filtering for refocus can be as efficient or even more efficient than FReD under some imaging conditions, as demonstrated by the computer-simulated results in this paper. The post-filter can be pre-calculated from a theoretical derivation of the curvature effect. The conclusion is that the new polar formatting with post filtering algorithm (PF2) should be considered as a viable candidate for a spotight-mode image formation processor when curvature effects are present.

1. Introduction and Problem Statement

The classic approach to SAR image formation from phase history data collected in the spotlight mode has been the polar formatting algorithm (PFA). In polar formatting, the collected phase history data are described in terms of a *slice* of the three-dimensional Fourier transform of the scene reflectivity data, obtained on a polar raster [1]. An inverse Fourier transform of these data (as projected onto a chosen two-dimensional plane) forms the SAR image. The derivation of this technique relies upon a sometimes unrealistic assumption of strictly planar wavefronts in the transmitted microwave pulses. Any actual amount of curvature present in these wavefronts introduces two forms of distortion into the SAR image as formed by the polar-format processor. First, there is a geometric distortion, which takes on the form of a keystone.[1] This distortion can be rectified in a straightforward manner by appropriate post-warping of the image. The second form of distortion is a space-variant defocusing effect, which can be shown to be one-dimensional in the cross-range direction, with a corresponding aperture phase function that is quadratic. The magnitude of this quadratic phase error term is a function of the range and cross-range position of the target, and becomes greater for those targets placed further in range and cross-range from the scene center. Figure 1 shows a real SAR image with these effects of wavefront curvature simulated. This 1K x 1K image represents a portion of a much larger scene that was illuminated and formed by the PFA algorithm. In this case, the image segment lies near the extreme cross-range edge of the larger scene, along the center range line. The space-variant defocus effects are clearly evident here. (The geometric distortion is not apparent across this smaller image segment at the edge of the larger scene imaged.)

[1] See [1], pp. 361-363.

DISCLAIMER

The usual approach to this situation has been simply to limit the size of the scene reconstructed, so that the effects of wavefront curvature are never realized. That is, it can be shown that by limiting the reconstructed image patch size to:

$$D \leq 2\rho_x \sqrt{\frac{2r_0}{\lambda}} \tag{1}$$

where D is the diameter of the scene patch, r_0 is the range from the radar to the scene center, and λ is the radar wavelength, the amount of quadratic phase error for any target in the scene will be held to less than $\pi/4$ radians, resulting in only a negligible amount of smearing in the formed image[2].

In this paper, we show that the above restriction on image scene size can be lifted by performing appropriate post-processing that removes the wavefront curvature defocusing effects. More importantly, we demonstrate that the computational burden required by this image restoration procedure is not particularly severe, at least for a certain set of imaging scenarios, in which it can be as little as only 25% of the polar-format image formation time. The key concept is to implement a space-variant one-dimensional image-domain filter, based upon an analytic derivation of the quadratic phase error that is induced by the curved wavefronts.

2. Filter Implementation

In [1], it is shown that the defocus effect of wavefront curvature on a spotlight-mode SAR image formed with polar formatting is a space-varying one that occurs in the cross-range (azimuth) direction only, at least for the condition wherein the SAR collection is obtained at broadside, and the standoff range is large compared with the diameter of the scene reconstructed. Under this assumption, the Fourier transform of the blur function can be shown to be phase-only and is given by[3]:

$$H(X) = \frac{x_0^2 - y_0^2}{2r_0 k_0} X^2 \tag{2}$$

where $k_0 = 4\pi/\lambda$, r_0 is the standoff range of the radar platform, (x_0, y_0) is the location of a target in the reconstructed slant-plane image, and X is the phase-history (Fourier transform domain) frequency associated with the cross-range image dimension. Note that this phase error function is quadratic in X.

By applying an appropriate spatially-varying filter to the image that is formed by the polar-format processer, the defocus effects induced by the expression of Equation 2 can be compensated. The filter is one-dimensional and applied in the cross-range direction. For a given location in the image, the length of the filter must be chosen sufficiently long to accommodate the support (width of) the defocus blur, which becomes most severe at the extreme range and cross-range locations in the image, i.e., the worst blurs occur at $(x_{max}, 0)$ and at $(0, y_{max})$, where x_{max} and y_{max} are the extreme values of cross-range and range in the image patch. If the filter were changed at every pixel, in strict accordance with the expression of Equation 2, the computational burden associated with filter implementation could become excessive. Fortunately, the filtering procedure can be made considerably more efficient than this by varying the filter function only as rapidly as required to maintain the residual blur at an acceptable level. Here, we will use the following criterion for acceptable residual blur: the quadratic phase correction term should be in error by no more than $\pi/4$ radians for any point in the reconstructed image (This is the

[2] See [1], pp. 95-97.
[3] See [1], pp. 361 - 363.

same criterion used to establish Equation 1 for the maximum size image patch that can be reconstructed without post-filtering correction.) Figure 2 shows a block diagram of the processing steps that constitute the polar formatting with post-filter correction algorithm (PF2).

3. Results from the PF2 Algorithm on Computer-Simulated SAR Data

In this section we demonstrate the utility of the new image formation algorithm on computer-simulated SAR phase history data. Consider a particular spotlight-mode SAR imaging geometry with the following parameters:

SAR parameter	**symbol**	**value**
wavelength	λ	0.06 m
cross-range resolution	ρ_x	0.33 m
range resolution	ρ_y	0.33 m
stand-off range	r_0	10,000 m
image patch size	D	1000 m
image size	N	4096 x 4096 pixels

Table 1: Parameters used in generation of synthetic SAR phase history data

For these parameters, note that Equation 1 predicts that the maximum scene patch diameter that would be free of wavefront curvature defocus effects would be 381 meters. As a result, we would definitely expect to see degradations in targets placed near the extreme range and cross-range positions of the 1000 m scene. We next use a synthetic target generator to calculate the exact phase history data that would be collected in the spotlight-mode from a SAR platform operating with the above parameters. Figure 3(a) shows nine targets as reconstructed by polar formatting (PFA) without the post-filtering applied. These targets are located at the scene center and eight extreme locations in range and cross-range across the scene patch. Note that the target at the scene center as well as the four targets at the scene corners are not defocused at all, as is predicted by Equation 2, since for all of these locations we have $x_0^2 - y_0^2 = 0$. Figure 3(b) shows the PFA reconstruction of a dense array of 128 x 128 image pixels with point targets placed on 8 pixel centers. This array is located on the center range line of the scene, at the extreme cross-range edge of the scene patch. Equation 2 predicts that the maximum defocus (largest quadratic phase term) occurs here (as well as at the extreme range position, $(0, y_{max})$). The two effects of the wavefront curvature, namely the geometric "sagging" distortion as well as the cross-range blurring of the targets, are clearly in this image. Figure 3(c) shows the result of reconstructing the same phase history data using the PF2 algorithm. In this case, the filter size was chosen to be 32 (cross-range) pixels wide, based on evaluation of the maximum rate of variation of the quadratic phase error function in the cross-range direction. (As described in the previous section, the criterion used here is that the amount of quadratic phase should not be in error by more than $\pi/4$ radians for any point inside the filter box, so that we guarantee negligible residual blurring.) The filter function was changed every 16 cross-range pixels, and on every range pixel. (The overlap in cross-range is required to correctly focus targets at the edge of the filter box.) Note that the targets are now well-focused and the geometric distortion has been removed. For this imaging scenario, the PF2 algorithm took 569 seconds to reconstruct the 4096 x 4096 image on a SUN Ultra 2 workstation, where the code was written in FORTRAN. The post-filtering portion of the algorithm represented only an additional 25% of the time to perform the conventional polar formatting, i.e., polar-to-rectangular interpolation followed by 2-D Fourier transformation.

4. Comparative Results from Range Migration Processing

In this section we compare the results of two range migration image formation algorithms to the results obtained from PF2 in the previous section. These algorithms are the RMA (range migration algorithm) described in [2], and the FReD (Frequency Domain Replication and Downsampling) algorithm, described in [3]. Both algorithms are based upon the original work of Prati, Rocca, et. al. (see [4], [5], and [6]) Flow diagrams showing the processing steps involved in both of these techniques are given in Figures 4 and 5. One of the drawbacks of the RMA algorithm is that it requires the phase history data to be upsampled in the along-track dimension at a rate that depends upon the collection geometry. For some imaging scenarios, such as those involving significant squint angles, the time to compute the upsampled data may be quite large. The FReD algorithm was developed to avoid the upsampling requirement, and hence render migration processing reasonably efficient in these situations. For the case simulated here, the required upsampling ratio for RMA was approximately 2:1. As shown in Table 2 below, the PF2 and FReD algorithms take similar amounts of time to complete the image formation, with PF2 being somewhat faster, while RMA takes roughly twice as long.

Algorithm	**Execution time (seconds)**
PF2	569
RMA	1153
FReD	713

Table 2: Execution times for the three algorithms as implemented in FORTRAN on a SUN Ultra 2 Workstation

5. Conclusions and Suggestions for Future Work

We have demonstrated that the traditional polar formatting algorithm for spotlight-mode SAR image formation, PFA, can be modified by addition of a space-variant post filter to accommodate the effects of wavefront curvature. The geometric distortion term is easily handled with a simple warping operation, but the space-variant filter is required to remove the residual quadratic phase defocusing that is induced by non-planar wavefronts. Our FORTRAN implementation of the new algorithm, PF2, would indicate that it is more computationally efficient than the original version of the seismic migration technique, RMA, and even more efficient than the migration processing version known as FReD, that avoids the need for along-track upsampling. Of course, these FORTRAN timings are not the final word on algorithm efficiency. A careful operations count needs to be performed to further investigate the relative computational merits of these techniques.

The question of how any of these techniques can be applied to spotlight-mode SAR image collection geometries other than broadside need to be studied. It should be possible to derive a more general version of Equation 2 that is applicable to squint mode, as well as to non-straight-line flight path collections. RMA becomes problematic at large squint angles, because the along-track upsampling demands under these conditions is severe. It is not clear at this point whether or not RMA or FReD can be applied to non-straight-line collections. A comparison of these, as well as other algorithms that can accommodate wavefront curvature, e.g., the class of techniques known as "overlap subaperture processing", should be conducted to cover all realistic imaging modalities.

6. Acknowledgments

The authors would like to thank Perry Gore who produced the artwork. This work was supported by the United States Department of Energy under Contract DE-AC04-94AL85000.

7. References

[1] Jakowatz, Charles, et. al, **Spotlight-Mode Synthetic Aperture Radar: A Signal Processing Approach**, Kluwer Academic Publishers, Boston, 1996.

[2] W. Carrara et al., **Spotlight Synthetic Aperture Radar: Signal Processing Algorithms**, Artech House, Boston, 1995.

[3] A. Golden, et. al., "Migration processing of spotlight SAR data", *Proceedings of SPIE*, Vol. 2230, pp.25-35, 1994.

[4] C. Pratti, et. al., "Spot Mode SAR Focusing with the ω-K Technique", *IEEE IGARSS*, pp. 631-634, 1991.

[5] C. Pratti and F. Rocca, "Focusing SAR Data with Time-Varying Doppler Centroid", *IEEE Trans. on Geoscience and Remote Sensing*, Vol. 30, No. 3, pp. 550-559, May, 1992.

[6] C. Cafforio, C. Prati, and F. Rocca, "SAR Data Focusing Using Seismic Migration Techniques," *IEEE Trans. on AES*, Vol. 27, No. 2, pp. 194-206, March, 1991.

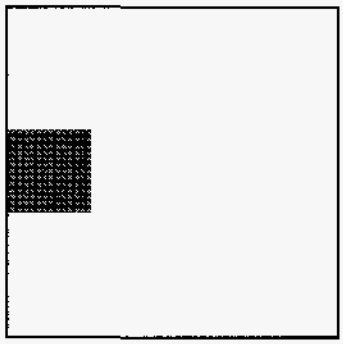

(a)

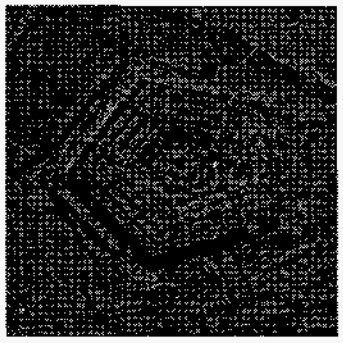

(b)

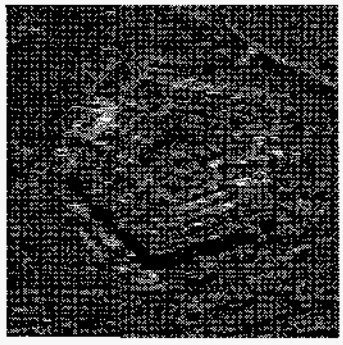

(c)

Figure 1: Real spotlight mode image with wavefront curvature effects simulated: (a) This 1K x 1K image patch lies at the extreme cross-range edge of the larger scene imaged. (b) The SAR image segment that would be reconstructed in the absence of wavefront curvature effects. (c) The image reconstructed by the polar formatting algorithm (PFA) when significant wavefront curvature is present. The effects of space-variant defocus can be clearly seen. The geometric distortion is not evident, because this is a small portion of the larger scene.

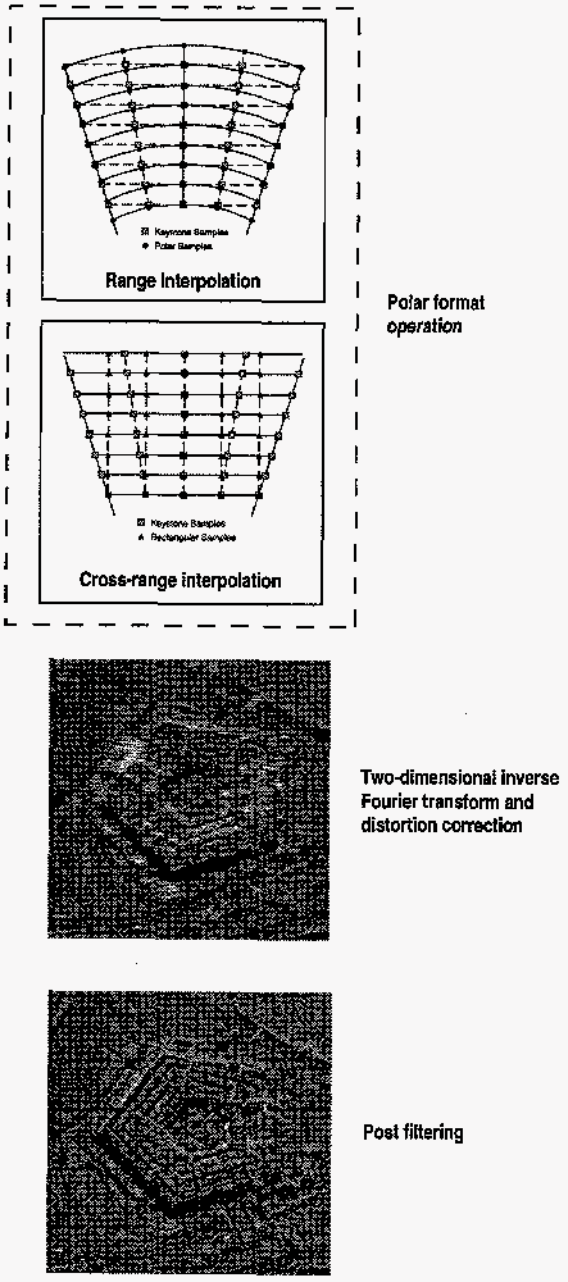

Figure 2: Processing steps for the polar-formatting with post-filtering algorithm (PF2).

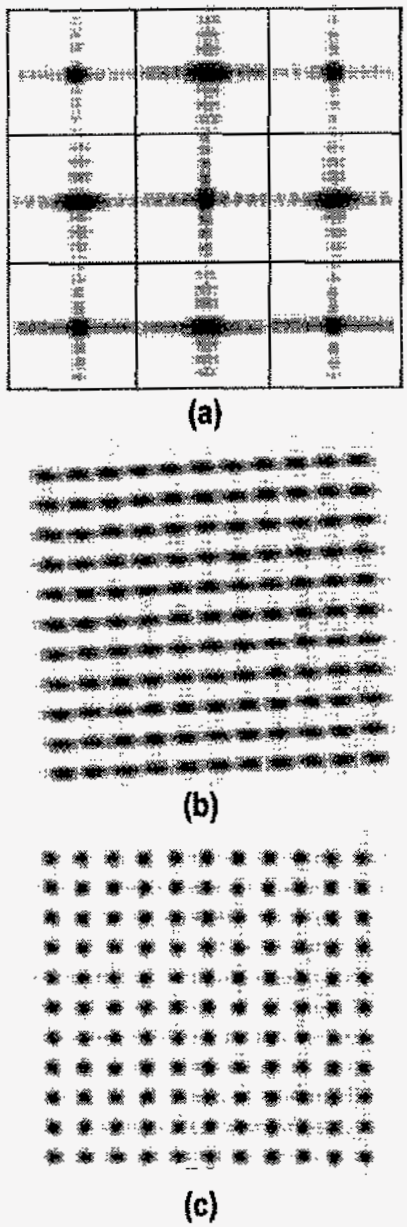

Figure 3: (a) Detail of targets reconstructed at center and eight extreme locations of scene patch with conventional polar format (PFA) processing. Note that targets at the scene center as well as at the corners of the patch are not defocused, as predicted by Equation 2. (b) PFA reconstruction of dense array of targets located at extreme cross-range edge of the scene patch. Note the cross-range blurring as well as the geometric distortion ("sagging") due to the effects of wavefront curvature. (c) Image reconstructed using PF2 algorithm. Note that geometric distortion as well as defocus effects are successfully removed.

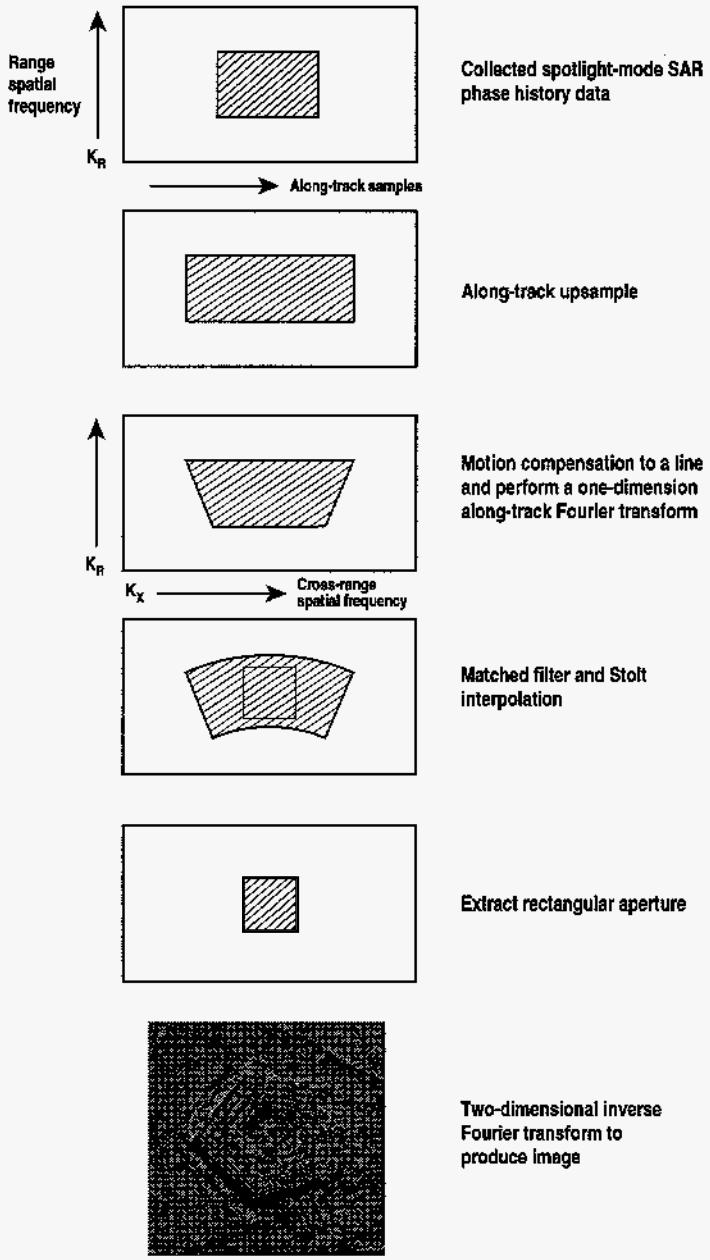

Figure 4: Processing steps for RMA algorithm

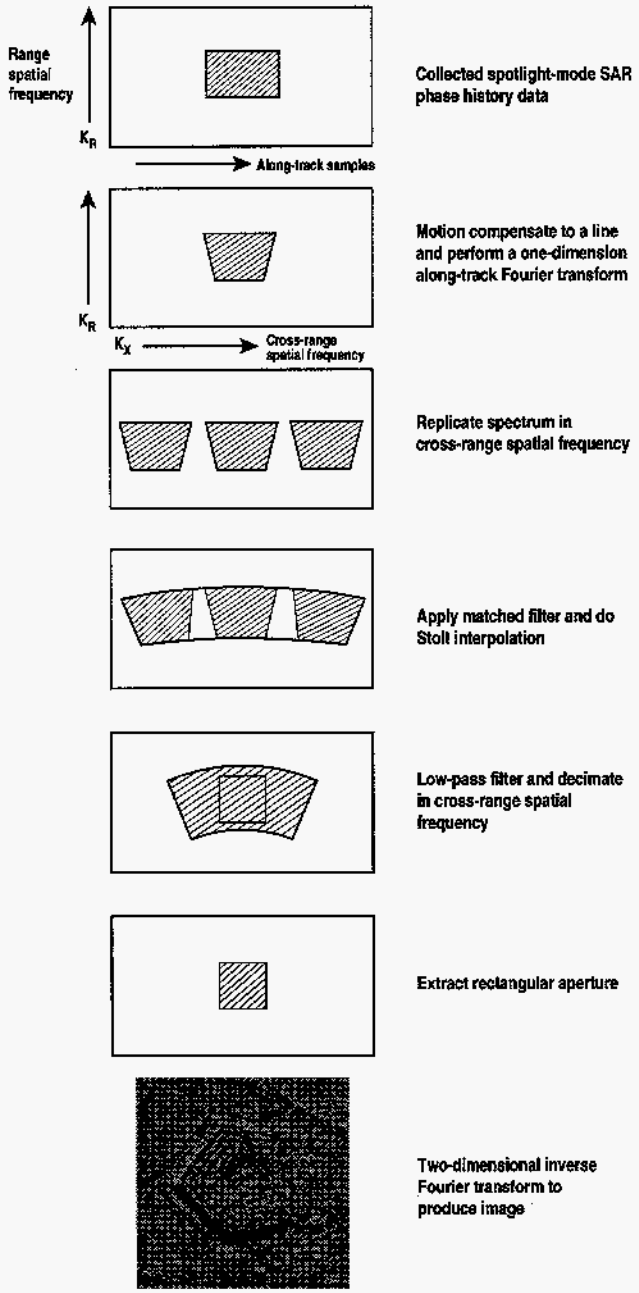

Figure 5: Processing steps for FReD algorithm